*Third International Conference on CFD in the Minerals and Process Industries*
*CSIRO, Melbourne, Australia*
*10-12 December 2003*

# DETAILED COMPUTATIONAL AND EXPERIMENTAL FLUID DYNAMICS OF FLUID BEDS

**N.G. DEEN, M. VAN SINT ANNALAND, and J.A.M. KUIPERS**

Faculty of Science and Technology, University of Twente,
P.O. Box 217, 7500 AE Enschede, THE NETHERLANDS

## ABSTRACT

To describe the hydrodynamic phenomena prevailing in large industrial scale fluidised beds continuum models are required. The flow in these systems depends strongly on particle-particle interaction and gas-particle interaction. For this reason proper closure relations for these two interactions are vital for reliable predictions on the basis of continuum models. Gas-particle interaction can be studied with the use of the lattice Boltzmann model, while the particle-particle interaction can suitably be studied with a discrete particle model. In this work it is shown that the discrete particle model has the capability to generate insight and eventually closure relations in processes such as mixing, segregation and homogeneous fluidisation.

## NOMENCLATURE

| | |
|---|---|
| $A$ | Hamaker constant |
| $C_d$ | drag coefficient, - |
| $d$ | diameter, *m* |
| $D$ | distribution function |
| $\mathbf{g}$ | gravitational acceleration, $m/s^2$ |
| $m$ | mass, *kg* |
| $M$ | image magnification, - |
| $N$ | number, - |
| $p$ | pressure, $kg/(m \cdot s^2)$ |
| $\mathbf{r}$ | position, *m* |
| $r$ | particle radius, *m* |
| $\mathbf{s}$ | volume-averaged displacement, *m* |
| $\mathbf{S}_p$ | particle drag sink term, $kg/(m^2 \cdot s^2)$ |
| $S$ | inter-surface distance between two spheres, *m* |
| $t$ | time, *s* |
| $\mathbf{u}$ | gas velocity, *m/s* |
| $\mathbf{v}$ | particle velocity, *m/s* |
| $V$ | volume, $m^3$ |
| $\mathbf{x}$ | coordinate vector, *m* |

### Greek symbols

| | |
|---|---|
| $\beta$ | inter-phase momentum transfer coefficient, $kg/(m^3 \cdot s)$ |
| $\varepsilon$ | porosity, - |
| $\rho$ | density, $kg/m^3$ |
| $\boldsymbol{\tau}$ | stress tensor, *Pa* |
| $\boldsymbol{\Phi}$ | flux, $kg/(m^2 \cdot s)$ |

### Subscripts

| | |
|---|---|
| 2D | two-dimensional |
| a | particle a |
| bf | background fluidisation |
| Br | bright pixel |
| cell | cell |
| Da | dark pixel |
| mf | minimum fluidisation |
| p | particle |
| s | solid phase |
| sf | spout fluidisation |
| Sh | shaded pixel |

## INTRODUCTION

In many industrial applications of dense gas-solid fluidised beds mixing and segregation phenomena are very important. For example, in gas-phase polymerisation reactors good mixing is essential to avoid hot spots due to the heat released by the highly exothermic polymerisation reactions and segregation of the larger particles is used to collect the product particles at the bottom of the fluidised bed. The mixing and segregation behaviour of fluidised beds is largely determined by the bubble characteristics and bubble dynamics.
Another example can be found in the application of spout fluid beds. These systems are frequently used in the process of granulation. In that process the obtained particle size distribution is largely determined by the operating regime occurring in the spout fluid bed. In order to control the particle size distribution and consequently reduce recycle streams, it is important to have a detailed understanding of the behaviour of particles near the spout region.
To model systems like those described in these two examples a multi-level modelling approach can be adopted, which is illustrated in Figure 1. The idea of this approach is to use different levels of modelling, each developed to study phenomena that occur at a certain length scale. Information obtained at the level of small length scales can be used to provide closure information at the level of larger length scales.

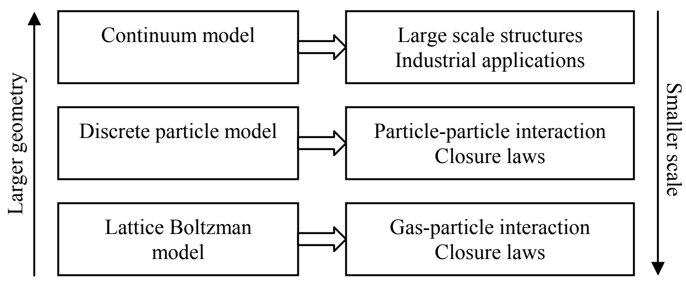


**Figure 1:** Multi-level approach for modelling of gas-particle flows. For each level of modelling the typical application area is indicated.

As indicated in Figure 1, continuum models are required to describe the hydrodynamic phenomena prevailing in large industrial scale systems. In the continuum model both the gas and particulate phases are described as interpenetrating fluids. Continuum models often use the Kinetic Theory of Granular Flow (KTGF) to provide closure equations for the internal momentum transport in the particulate phase. Although these Euler-Euler models have been developed and studied extensively in the literature (Gidaspow, 1994, Simonin, 1996, Kuipers and Van Swaaij, 1998, Goldschmidt, 2001), these models still lack the capability of describing quantitatively mixing and segregation rates in poly-disperse fluidised beds.

Direct experimental validation of the continuum models in large scale systems is difficult and cumbersome, since only macroscopic phenomena are accessible, such as macroscopic velocity profiles, bubble size distributions, etc., which result, however, indirectly from microscopic interactions between the particles and the particles with the gas phase. In Discrete Particle Models (DPM), where each particle is tracked individually, detailed collision models can be incorporated, rendering the DPM a valuable research tool to validate the underlying assumptions in the KTGF concerning the particle-particle interactions and the particle velocity distribution functions (see a.o. Goldschmidt, 2001).

The interaction between the gas and the particles is another important element in the continuum approach, which requires closures. There are a number of semi-empirical closure relations available, which although they are widely applied contain a large uncertainty, which has a significant effect on the overall behaviour of the fluidised bed. Techniques such as the lattice Boltzmann model (LBM) (see Figure 1) can be used to validate and eventually improve these closure relations. In LBM the flow around small ensembles of particles can be modelled, without making prior assumptions such that the gas-particle interaction can be quantified.

In this work we will focus on the level of the DPM. The capabilities of this model will be illustrated by the determination of operating regimes in a spout fluid bed, mixing and segregation in a fluid bed, and a study of the influence of the van der Waals force on the homogeneous fluidisation of small particles.

First the numerical model will briefly be explained. Then two experimental techniques, particle image velocimetry and digital image analysis, will be introduced, which are used to obtain detailed information about the particle behaviour.

## NUMERICAL MODELING

The discrete particle model used in this work is based on the hard-sphere and soft-sphere models developed by Hoomans (1996, 2000). A short description of the model is given in this section, for details the interested reader is referred to the work of Hoomans (1996, 2000) and Tsuji *et al*. (1993).

Particle collision dynamics are described by collision laws, which account for energy dissipation due to non-ideal particle interaction by means of the empirical coefficients of normal and tangential restitution and the coefficient of friction.

The particle collision characteristics play an important role in the overall bed behaviour as was shown by Goldschmidt *et al.* (2001). For this reason the collision properties of the particles used for the experimental validation were accurately determined by detailed impact experiments and supplied to the model.

The motion of every individual particle in the system is calculated from the Newtonian equation of motion:

$$m_p \frac{d\mathbf{v}_p}{dt} = -V_p \nabla p + \frac{V_p \beta}{1-\varepsilon}(\mathbf{u} - \mathbf{v}_p) + m_p g$$

where β represents the inter-phase momentum transfer coefficient.

The gas phase hydrodynamics are calculated in two dimensions from the volume-averaged Navier-Stokes equations:

$$\frac{\partial}{\partial t}(\varepsilon \rho_g) + \nabla \cdot (\varepsilon \rho_g \mathbf{u}) = 0$$

$$\frac{\partial}{\partial t}(\varepsilon \rho_g \mathbf{u}) + \nabla \cdot (\varepsilon \rho_g \mathbf{u}\mathbf{u}) = -\varepsilon \nabla p - \nabla \cdot (\varepsilon \boldsymbol{\tau}) - S_p + \varepsilon \rho_g \mathbf{g}$$

The two-way coupling between the gas-phase and the particles is achieved via the sink term $\mathbf{S}_p$, which is computed from:

$$S_p = \frac{1}{V_{cell}} \int \sum_{a=0}^{N_p} \frac{V_a \beta}{1-\varepsilon}(\mathbf{u} - \mathbf{v}_a) D(r - r_a) dV$$

The distribution functions *D* distributes the reaction force acting on the gas phase to the Eulerian grid.

## EXPERIMENTS

In order to validate the discrete particle model two experimental techniques are used in this work: particle image velocimetry and digital image analysis. These two techniques are introduced in the following sections.

### Particle image velocimetry

Particle image velocimetry (PIV) is a non-intrusive technique for the measurement of an instantaneous velocity field in one plane of a flow. In traditional PIV the flow is visualized by seeding it with small tracer particles that perfectly follow the flow. In gas-particle flows, the discrete particles can readily be distinguished, so no additional tracer particles are needed to visualize the particle movement. The flow in the front of the bed is illuminated with the use of halogen lamps. A CCD camera is used to record images of the particles in the illuminated plane. Two subsequent images of the flow, separated by a short time delay, $\Delta t$, are divided into small interrogation areas. Cross-correlation analysis is used to determine the volume-averaged displacement, $\mathbf{s}(\mathbf{x}, t)$, of the particle images between the interrogation areas in the first and second image. The velocity within the interrogation area is then easily determined by dividing the measured displacement by image magnification, *M*, and the time delay:

$$\mathbf{v}_p(\mathbf{x}, t) = \frac{\mathbf{s}_p(\mathbf{x}, t)}{M \Delta t}$$

provided that $\Delta t$ is sufficiently small. Further details on the theoretical background of PIV can be found in the work of Westerweel (1997). An overview of the status and trends of PIV applied to two-phase flows can be found in the work of Deen *et al*. (2002).

#### Digital image analysis

In this work a digital image analysis (DIA) technique is employed to detect bubbles in fluidised beds based on the absolute intensity level (brightness) of pixels. Agarwal *et al.* (1996) first used a digital image analysis technique to detect bubbles in a bubbling fluidised bed. Goldschmidt (2001) improved this technique by developing a procedure to compensate for the effect of the aperture of the camera on the brightness of the pixels.

The digital images are divided into the same interrogation areas as are used for PIV. All pixels in an interrogation area are assigned to one of three categories. The first category consists of bright pixels and is characteristic for particles that are close to the front wall constituting the dense region in the bed. The second category contains shaded pixels, which are characteristic for particles deeper in the bed that are shaded by surrounding particles causing the brightness to decrease. The occurrence of shaded particles implies that particles are present but not in a dense region. Dark pixels form the last category and are characteristic for the background of the bed, i.e. very low brightness.

For each interrogation area the 2D particle fraction, $\varepsilon_{s,2D}$, is calculated using:

$$\varepsilon_{s,2D} = \frac{N_{Br}\varepsilon_{Br} + N_{Sh}\varepsilon_{Sh} + N_{Da}\varepsilon_{Da}}{N_{Br} + N_{Sh} + N_{Da}}$$

where $N$ represents the number of pixels in an interrogation area belonging to each of the three categories. The particle fraction for each category ($\varepsilon_{Br}$ = 0.8; $\varepsilon_{Sh}$ = 0.4; $\varepsilon_{Da}$ = 0.0) was determined by calibration of a single image. $\varepsilon_{s,2D}$ is extended to 3 dimensions and converted into the void fraction:

$$\varepsilon = 1 - \left(\varepsilon_{s,2D}\right)^{\frac{3}{2}}$$

By applying PIV and DIA simultaneously, the measured particle velocity and the particle volume fraction can be used to calculate particle flux maps, which can be used to compare with numerical simulations.

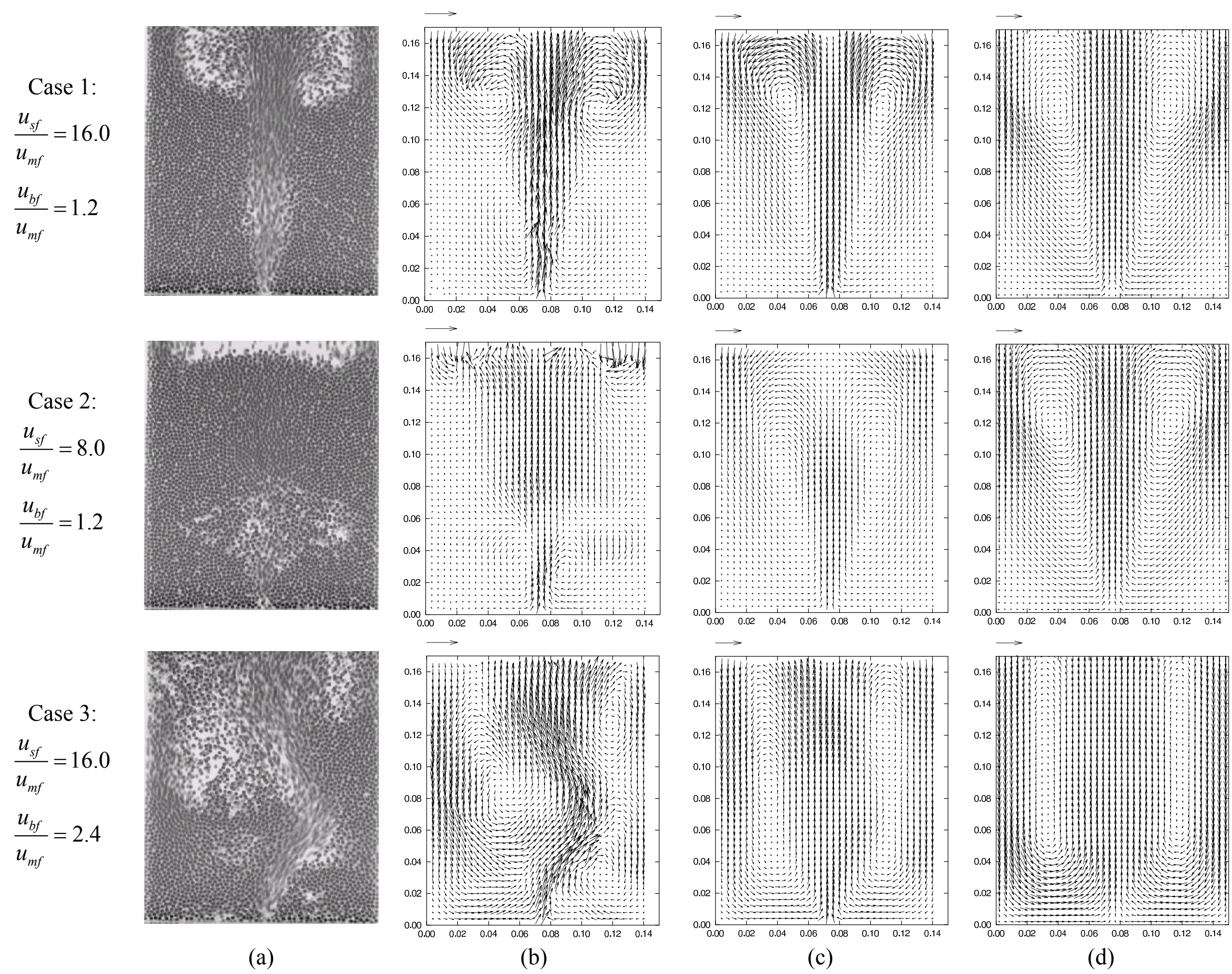


**Figure 2**: Instantaneous snapshots (a) and associated particle velocity maps (b) of experiments performed at different operating regimes. The reference vector of the velocity maps represents a particle velocity of 1.0 m/s. The snapshots are inverted to improve visibility. Experimental (c) and simulated (d) time-averaged particle flux maps for different operating regimes. The reference vector of the flux maps represents a particle flux of 842 kg/(m$^2$·s). The position in the bed is given in m along the axes.

## RESULTS

In this section the capabilities of the discrete particle model will be demonstrated with four different examples. The first example involves the identification of flow regimes of gas-particle flow in a spout fluid bed. In the second and third example, the process of mixing and segregation will be considered. Finally the influence of the van der Waals force in systems with small particles will be discussed.

### Regime identification in a spout fluid bed

Link *et al*. (2003) carried out PIV and DIA experiments along with simulations with the discrete particle model to investigate the flow in a pseudo 2-dimensional spout fluid bed containing Geldart D particles. Three different operating conditions were used: a base case (Case 1), a reduced spout velocity case (Case 2) and an increased background fluidisation velocity case (Case 3). The results of the three different cases are shown in Figure 2. It is observed that when the average gas velocity is increased the absolute value of the particle fluxes increases. This is due to an increase of the total drag force exerted by the gas on the particles because of a larger velocity difference between the particles and the gas.

When the spout velocity is reduced the spout penetration depth decreases and the particle flux generated by the spout also decreases. A lower spout velocity results in a lower velocity difference between the particles and the gas and consequently to a lower drag force.

When the background fluidisation velocity is increased the average flow pattern changes dramatically. The width and height of the area influenced by the spout is increased, resulting in high values for the particle fluxes in the entire bed. Instantaneous images, like the ones displayed in Figure 2b, show that these profiles are the result of the spout moving from left to right and back. This oscillating behaviour is caused by the gas bubbles that are produced alongside the spout at higher background fluidisation velocities.

When the spout velocity is reduced the behaviour of the bed hardly changes. Even at this low spout velocity the spout penetrates through the entire bed. This could explain the limited influence of the spout velocity on the bed behaviour.

When the background fluidisation velocity is increased the influence on the bed behaviour is similar to the effects observed experimentally.

In general it is observed that the DPM is able to reproduce the different regimes occurring in a spout fluid bed. There are still some quantitative differences, which may be due to the closure model that is used for the drag force. The influence of the drag force will be demonstrated in the following example.

### Single bubble injected in a fluidised bed

As indicated in the introduction the processes of mixing and segregation in fluidised beds are largely determined by the bubble characteristics and bubble dynamics. Bokkers *et al*. (2003) used the discrete particle model to investigate the role of bubbles in a fluidised bed. They studied the influence of the drag force on the bubble formation in a fluidised bed filled with Geldart B particles. In their work, the inter-phase momentum transfer coefficient, $\beta$ is modelled in two ways. In the first model, the dense regime ($\varepsilon < 0.80$) the Ergun equation (1952) is used, whereas in the more dilute regime ($\varepsilon > 0.80$) $\beta$ is calculated with the use of the correlation of Wen and Yu (1966).

In the second model the drag relations proposed by Koch and Hill (2001) are applied. This drag model was based on the simulations with the lattice Boltzmann model and does not suffer from experimental inaccuracies.

In Figure 3 the bubble size at 0.2 s after the start of the jet as predicted by the DPM is compared with the experiment. It is seen that when the first drag model is used, the predicted bubble size is much larger than observed in the experiment. The first model tends to overpredict the drag, which prevents the particles from raining through the roof of the bubble. It is seen that the second drag model, shows a better correspondence with the experimental image. The size and shape of the bubble as well as the raining phenomenon are predicted correctly.

Subsequently the particle velocity profiles simulated with the DPM using the Koch and Hill drag relations have been compared with PIV measurement data, depicted in Figure 4. The figure demonstrates that the PIV technique has been applied successfully to obtain the local instantaneous ensemble averaged particle velocity field in a dense gas-solid fluidised bed. Furthermore, when comparing the DPM results with the PIV data, it can be concluded that the DPM predicts the particle streamlines very nicely. Only the magnitude of the particle velocities just above the bubble is somewhat overestimated in the DPM, probably due to an underestimation of the gas-wall friction.

### Segregation in a freely bubbling fluidised bed

In the previous section, mixing induced by a single injected bubble has been studied. In this section the rates of segregation of a binary mixture of particles in a freely bubbling fluidised bed predicted by the DPM have been compared with a set of segregation experiments carried out with the digital image analysis by Goldschmidt (2001). It is noted that these simulations have been carried out with the hard-sphere collision model for 12 s simulation time with a superficial gas velocity just above the minimum fluidisation velocity of the mixture, which is very CPU demanding.

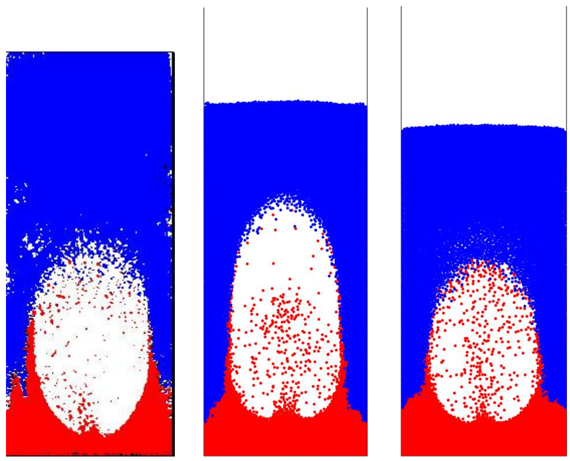

(a) Experiment (b) DPM Ergun/Wen & Yu (c) DPM Koch & Hill

**Figure 3**: Bubble shape 0.2 s after injection in a mono-disperse fluidised bed: Comparison of experiment with DPM using different drag models.

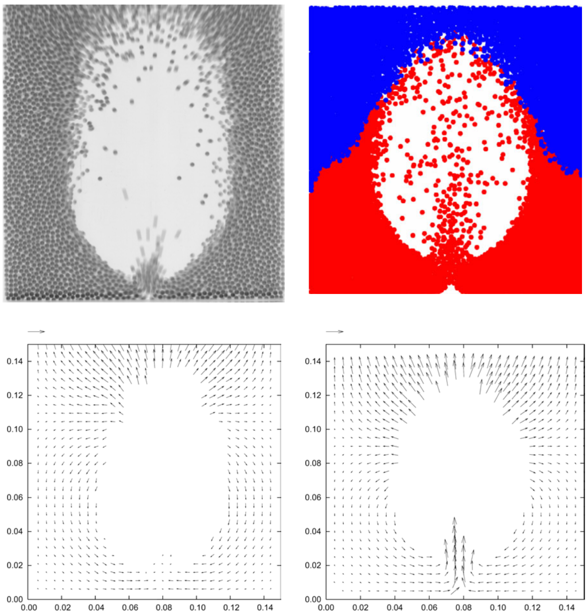



(a) Experiment (b) DPM, Koch & Hill

**Figure 4**: Snapshots and corresponding particle velocity maps of a single bubble at 0.150 s after injection in a mono-disperse fluidised bed: Comparison of the PIV results with DPM simulations using Koch & Hill drag closures. The reference vector corresponds with a particle velocity of 1 m/s.

To be able to compare segregation rates for different systems, the segregation is expressed on a relative scale, ranging from 0 (ideal mixture) to 1 (complete segregation). As can be seen in Figure 5 the simulated relative segregation compares reasonably well with the experimentally observed relative segregation. Only the initial relative segregation is strongly overestimated due to the artificial initial positioning of the particles causing compaction of the bed, which enhances the initial segregation artificially. A second simulation was carried out with a different initial particle configuration. A well-mixed bed of the large and small particles was obtained using a high superficial gas velocity (2 m/s). With this initial condition the predicted segregation rates compare very well with the experimental findings. This result indicates the importance of the initial particle configuration on the initial segregation rates.

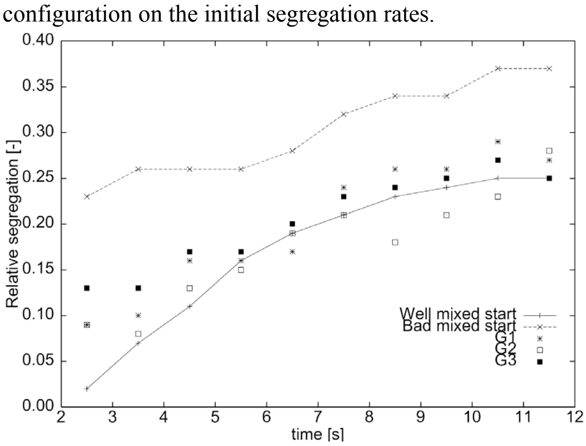



**Figure 5**: Relative segregation in a freely bubbling bed for a binary mixture: effect of initial particle configuration (45660 particles, 25 mass% small, $U_{bg}$ = 1.3 m/s, hard-sphere collision model, Ergun/Wen&Yu drag closures; G1-G3: experiments carried out three times).

**Van der Waals force in Geldart A particles**

In flows with small particles (Geldart A particles, typically 20-100 μm), the homogeneous fluidisation regime is extended as compared with flows with larger particles. This phenomenon cannot be explained by the drag or non-ideal particle-particle collisions. In this case, the van der Waals forces acting between particles are the dominant process for the occurrence of homogenisation.

Ye *et al*. (2003) demonstrated the effect of the van der Waals force by adding an additional force term into the equation of motion of the particles. To calculate the inter-particle van der Waals forces, the Hamaker equation was adopted:

$$F_{vdW}(S) = \frac{A}{3}\frac{2r_1r_2(S+r_1+r_2)}{[S(S+2r_1+2r_2)]^2}\left[\frac{S(S+2r_1+2r_2)}{(S+r_1+r_2)^2-(r_1-r_2)^2}-1\right]^2$$

where $S$ is the intersurface distance between two spheres, $A$ the Hamaker constant, and $r_1$ and $r_2$ the radii of the two spheres respectively.

An example of the effect of the Van der Waals force on structure formation can be seen in Figure 6. It can be seen that for low Hamaker constants the Van der Waals force is weak and that bubbles are formed. For high Hamaker constants ($10^{-20}$ J) no bubbles are formed, however the particles form chain like structures.

## CONCLUSIONS

To describe the hydrodynamic phenomena prevailing in large industrial scale fluidised beds continuum models are required. The flow in these systems depends strongly on particle-particle interaction and gas-particle interaction. For this reason proper closure relations for these two interactions are vital for reliable predictions on the basis of continuum models. Gas-particle interaction can be studied with the use of the lattice Boltzmann model, while the particle-particle interaction can suitably be studied with a discrete particle model. In this work it is shown that the discrete particle model has the capability to generate insight and eventually closure relations in processes such as mixing, segregation and homogeneous fluidisation.

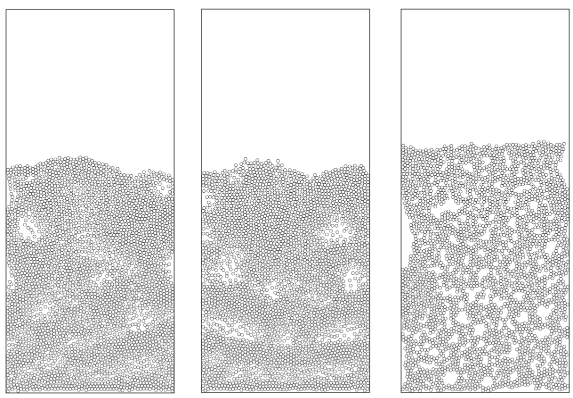

$A = 10^{-22}$ J $A = 10^{-21}$ J $A = 10^{-20}$ J

**Figure 6**: Demonstration of the influence of the van der Waals force on the meso-scale behaviour of Geldart A particles in a fluidised bed, for different values of the Hamaker constant.

## ACKNOWLEDGEMENTS

The authors would like to gratefully acknowledge G.A. Bokkers, J.M. Link, and M. Ye for their contribution to this work.


## REFERENCES


AGARWAL, P.K., A.S. HULL and K.S. LIM, (1997), "Digital Image Analysis Techniques for the Study of Bubbling Fluidized Beds", in "Non-invasive monitoring of multiphase flows", J. Chaouki, F. Larachi, M.P. Dudukovic, Elsevier Science B.V., Amsterdam, The Netherlands, 407-454.

BOKKERS, G.A., VAN SINT ANNALAND, M., and KUIPERS, J.A.M., (2003), "Mixing and segregation in a bi-disperse gas-solid fluidised bed: A numerical and experimental study", *Powder Technol.*, submitted for publication.

DEEN, N.G., WESTERWEEL J., and DELNOIJ, E., (2002), "Two-phase PIV of Bubbly Flows: Status and Trends", *Chem. Eng. Technol*, **25-1**, 97-101.

ERGUN S., (1952), "Fluid Flow through Packed Columns", *Chem. Eng. Prog.*, **48**, 89-94.

GIDASPOW, D., (1994), "Multiphase flow and fluidization: Continuum and kinetic theory descriptions", Academic Press, Boston.

GOLDSCHMIDT, M.J.V., (2001), "Hydrodynamic Modelling of Fluidised Bed Spray Granulation", PhD thesis, Twente University.

GOLDSCHMIDT, M.J.V., KUIPERS, J.A.M. and VAN SWAAIJ, W.P.M., (2001), "Hydrodynamic Modeling of Dense Gas-Fluidised Beds using the Kinetic Theory of Granular Flow: Effect of Coefficient of Restitution on Bed Dynamics.", *Chem. Eng. Sci.*, **56**, 571-578.

HOOMANS, B.P.B., KUIPERS, J.A.M., BRIELS, W.J. and VAN SWAAIJ, W.P.M., (1996), "Discrete Particle Simulation of Bubble and Slug Formation in a Two-Dimensional Gas-Fluidised Bed: A Hard-Sphere Approach", *Chem. Eng. Sci.*, **51**, 99-118.

HOOMANS, B.P.B., (2000), "Granular Dynamics of gas-solid two-phase flows", Ph.D. Thesis, University of Twente.

KOCH, D.L. and HILL, R.J., (2001), "Inertial Effects in Suspension and Porous-Media Flows", *Annu. Rev. Fluid Mech.*, **33**, 619-647.

KUIPERS, J.A.M. and VAN SWAAIJ, W.P.M., (1998), "Computational fluid dynamics applied to chemical reaction engineering", *Adv. Chem. Eng.*, **24**, 227-328.

LINK, J.M., ZEILSTRA, C., DEEN, N.G. and KUIPERS, J.A.M., (2003), "Validation of a discrete particle model in a 2D spout-fluid bed using non-intrusive optical measuring techniques", *Can. J. Chem. Eng.*, accepted for publication.

SIMONIN, O., (1996), "Modelling turbulent reactive dispersed two-phase flows in industrial equipments", In Proc. of the third world conference in applied computational fluid dynamics, Freiburg, Germany.

TSUJI, Y., KAWAGUCHI, T. and TANAKA, T., (1993), "Discrete Particle Simulation of Two Dimensional Fluidized Bed", *Powder Technol.*, **77**, 79-87.

WEN, Y.C. and YU, Y.H., (1966), "Mechanics of Fluidization", *Chem. Eng. Prog. Symp. Ser.*, **62**, 100-111.

WESTERWEEL, J., (1997), "Fundamentals of Digital Particle Image Velocimetry", *Meas. Sci. Technol.*, **8**, 1379-1392.

YE, M., VAN DER HOEF, M.A. and KUIPERS, J.A.M., (2003), "A Numerical Study of Fluidization Behavior of Geldart A Particles with Discrete Particle Model", *Powder Technol.*, submitted for publication.